

# Effect of molecular weight on the spherulitic growth rate of poly(aryl ether ether ketone)\*

Yves Deslandes, Frank-Nid Sabir† and Jacques Roovers

Division of Chemistry, National Research Council of Canada, Ottawa, Ontario,  
Canada K1A 0R9

(Received 29 March 1990; accepted 22 May 1990)

This study examines the change in spherulitic growth rate of poly(aryl ether ether ketone) (PEEK) as a function of molecular weight in the range of  $M_n = 6900$  to  $60\,200$  and for temperatures varying between  $250$  and  $300^\circ\text{C}$ . Optical microscopy using polarized light was used to follow the growth of the spherulites. Detailed analysis of the temperature dependence of the growth rates indicates that, within this relatively narrow range of molecular weight and temperature, both the pre-exponential factor and the exponential factor involving the free energy for nucleation are affected by molecular weight. Values of  $K_g$  increase with molecular weight from  $\approx 0.8 \times 10^6 \text{ K}^2$  to  $1.82 \times 10^6 \text{ K}^2$ . Values of  $\sigma_e$ , the end surface free energy, increase likewise from  $41$  to  $101 \text{ erg cm}^{-2}$  with increasing molecular weight. The results of the microscopy study and the differential scanning calorimetry study are compared and discussed in terms of the relevance of either a thermodynamic model or a kinetic model with regime behaviour for the kinetics of crystallization of PEEK.

(Keywords: poly(ether ether ketone); polymer crystallization; spherulitic growth; crystallization kinetics)

## INTRODUCTION

Poly(oxy-1,4-phenyleneoxy-1,4-phenylene-carbonyl-1,4-phenylene), more commonly referred to as poly(aryl ether ether ketone) or PEEK, is a high-temperature polymer that is becoming increasingly interesting as a thermoplastic matrix material in composites for engineering purposes. This semicrystalline polymer is characterized by a combination of attractive properties such as excellent thermal stability, outstanding chemical resistance and good fracture toughness<sup>1</sup>.

The crystallization kinetics of commercial PEEK samples have been extensively studied, particularly using d.s.c.<sup>2-9</sup>. However, because of the relatively high degree of nucleation observed with commercial samples and the consequent small dimensions for the spherulites, only a limited number of studies have been performed using optical microscopy. Blundell and Osborn<sup>2</sup> studied a special sample that had a low nucleation density, while Kumar *et al.*<sup>3</sup> were able to study a commercial sample. When comparing the two results, Kumar *et al.* found that the growth rate observed by them was three times higher than those reported by Blundell and Osborn. But, since accurate data on the molecular weight of the samples were not provided, this discrepancy cannot be explained. Deslandes *et al.*<sup>10</sup> were able to measure the radial growth rate of commercial PEEK, but only after keeping the polymer above the melting temperature for relatively long periods of time. It is believed that chemical and physical changes took place during the thermal processing and decreased both the crystal growth rate and the nucleation densities. This allowed an optical microscopy study, but on a material that had been modified by the thermal process.

No data exist in the literature about the effect of molecular weight on the radial growth rate as well as the overall crystallization kinetics of PEEK. This is due to the unavailability of a sufficient range of molecular weights from commercial sources. In this paper we report a study of the effect of molecular weight on the spherulitic growth rate based on a series of PEEK samples prepared in our laboratory<sup>11</sup>. A d.s.c. study of the same samples has been communicated in the previous paper<sup>12</sup>. The samples have number-average molecular weights varying between  $6900$  and  $60\,200$ . They exhibit relatively low nucleation densities, so that their crystallization can be studied by optical microscopy.

## EXPERIMENTAL

Samples used in this study were synthesized according to the method reported elsewhere<sup>11</sup>. Basically the method involved the preparation of 4,4'-difluorobenzophenone-ketimine, which was reacted with hydroquinone. The resulting poly(aryl ether ether ketimine) was then fractionated in benzene by addition of n-hexane. Molecular weights were determined by light scattering in tetrahydrofuran (THF). The polydispersity index was determined from size exclusion chromatography (s.e.c.) measurements. The fractions were then hydrolysed to produce PEEK. The samples have weight-average molecular weights ranging between  $8300$  and  $79\,500$ . Characteristics of the various fractions are reported in Table 1.

Specimens were prepared for growth rate measurement by placing the samples between a glass plate and a cover glass. The polymer (powder form) was melted at  $400^\circ\text{C}$  for  $1$  min before being placed in the hot stage heated to the desired temperature. This short period of time in the molten state was chosen because oxidation is known to

\* Issued as NRCC report no. 32526

† NRCC summer student 1988, Department of Chemical Engineering, Lakehead University, Thunder Bay, Ontario, Canada

**Table 1** Characteristics of the PEEK samples used in this study

Sample	$M_w$	$M_n$	$T_g$ (°C) <sup>a</sup>	$T_m$ (°C) <sup>b</sup>	$U^*$ (cal mol <sup>-1</sup> )	
					$T_\infty = T_g - 55$	$T_\infty = T_g - 30$
4D/1	79 500	60 200	150.6	404.0	4140	1775
1A22/1	55 500	34 900	149.4	401.9	4200	1825
4E/1	39 200	30 900	148.6	401.2	4560	1765
1B/1'	32 000	21 500	147.5	398.8	4560	1765
2C/1	18 000	14 500	145.3	395.0	4560	2145
1C/1	13 500	9 000	141	387.9	4560	2155
2D/1	8 300	6 900	137.9	382.2	4560	2145

<sup>a</sup>From d.s.c. at 10°C min<sup>-1</sup><sup>b</sup>Calculated: see text and ref. 12

occur in air at this temperature<sup>8</sup>. We realize that this short time may result in an incomplete destruction of the original nuclei, but no data on primary nucleation densities are acquired from this experiment. It is assumed, however, that the incomplete destruction of the original nuclei would not affect the radial growth of the spherulite. This assumption is supported by the work of other authors<sup>13</sup>.

Spherulitic growth rates were measured using a polarizing microscope to which were attached a Polaroid camera and a calibrated Mettler FP52 hot stage. The stage temperature can be varied between room temperature and 300°C and is constant to 0.1°C. Photographs of the spherulites were taken at different time intervals and their diameters determined with a calibrated measuring magnifier. Because of the limitation of our hot stage, no data are available for temperatures exceeding 300°C. The lowest  $T_c$  at which growth rate could be measured was 250°C. Below this temperature crystallization was too fast to be recorded. For the lower-molecular-weight samples, crystallization was too fast to be recorded below 280°C. By means of a fine thermocouple we have verified that the temperature equilibration of the sample in the hot stage takes less than 20 s. No data are recorded during the cooling in that interval, as shown in *Figures 1* and *2*. It has also been checked that the heat of crystallization does not affect the temperature of the hot stage.

Glass transition temperature ( $T_g$ ) was measured for each molecular weight using a DuPont differential scanning calorimeter model 1090, at a heating rate of 10°C min<sup>-1</sup> (ref. 12). The samples were first heated from 30 to 400°C, then rapidly removed from the d.s.c. cell and quenched in liquid nitrogen to make a totally amorphous sample. The  $T_g$  was then determined on the amorphous sample in a d.s.c. run from 30 to 400°C. The  $T_g$  was taken as the midpoint of the transition. The values of  $T_g$  are reported in *Table 1*.

## RESULTS

Two series of micrographs showing the development of the spherulites as a function of time are shown in *Figures 1* and *2*. It should be mentioned that the nucleation density was not the same for all samples. The samples 2C/1 and 2D/1 are characterized by a relatively low nucleation density, which facilitates the acquisition of the data, while the other samples show higher nucleation densities. Changes in nucleation densities are suspected

to be due to variation in the number of heterogeneous nuclei in the samples. No correlation between nucleation density and molecular weight was observed. It was also observed that the number of nuclei slightly decreased with increasing crystallization temperature. In all cases studied, the typical polarization cross of spherulites was observed.

The spherulitic growth rates  $G$  were found to be linear with respect to time during the early stages of growth. However, as crystallization progressed to a point where more than 50% of the field of view of the micrograph corresponded to crystallized polymer, a slight decrease in rate was observed. Consequently, only the rates measured at the early stage of growth were used in the calculations.

As expected, *Figure 3* confirms the decrease of the radial growth rate as the temperature increases from 250°C. This is in agreement with d.s.c. studies, which found that the maximum growth rate of PEEK occurs at around 230°C<sup>2,12</sup>. The curves in *Figure 3* also indicate a significant decrease in spherulitic growth rate as the molecular weight increases<sup>12</sup>.

It is possible to derive an empirical relationship between growth rate and molecular weight by selecting data in *Figure 3* at a constant temperature. Straight lines are obtained when the logarithm of the growth rate is plotted against the logarithm of the number-average molecular weight. *Figure 4* illustrates five of these curves, taken at 279, 283, 287, 291 and 295°C. Clearly, both the slopes and the intercepts of the lines change with temperature.

This molecular-weight dependence can be expressed by:

$$\log G(T_c) = \log A(T_c) + B(T_c) \log M_n \quad (1)$$

where  $A(T_c)$  and  $B(T_c)$  are both functions of the temperature of crystallization  $T_c$ . The slope  $B(T_c)$  varies from -2.7 to -3.5 between 279 and 295°C. A relationship between  $\log G(T_c)$  and  $\log M_w$  similar to ours was reported recently for poly(*p*-phenylene sulphide) by Lopez and Wilkes<sup>14</sup>, who studied polymer fractions having molecular weights varying between 24 000 and 63 000. Their slopes varied between -2.1 and -3.1.

Attempts to find a better fit using other expressions that have been proposed in the literature were not successful. Unsatisfactory coefficients of correlation were obtained when we used the formula proposed by Hoffman<sup>15</sup>, where the crystal growth is inversely proportional to the degree of polymerization. More

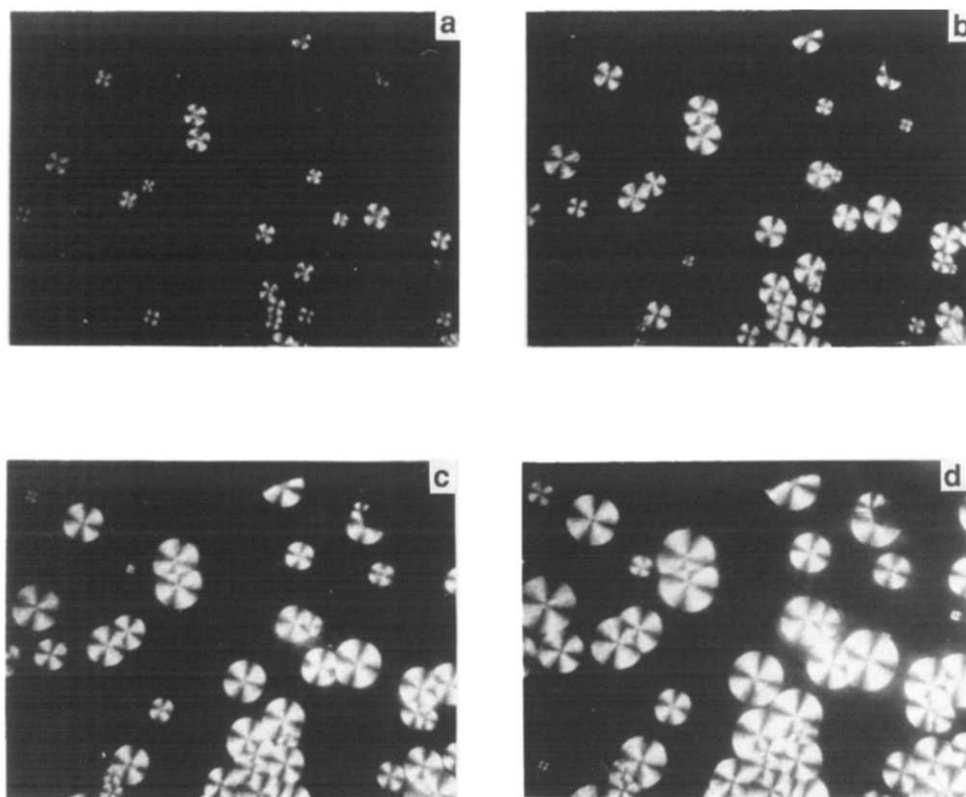


**Figure 1** Optical micrographs showing the evolution of spherulitic growth for the sample 2D/1 with  $M_n = 6900$  after 95 s (a), 100 s (b), 105 s (c) and 110 s (d).  $T_c = 298^\circ\text{C}$ ; scale bar =  $200\ \mu\text{m}$

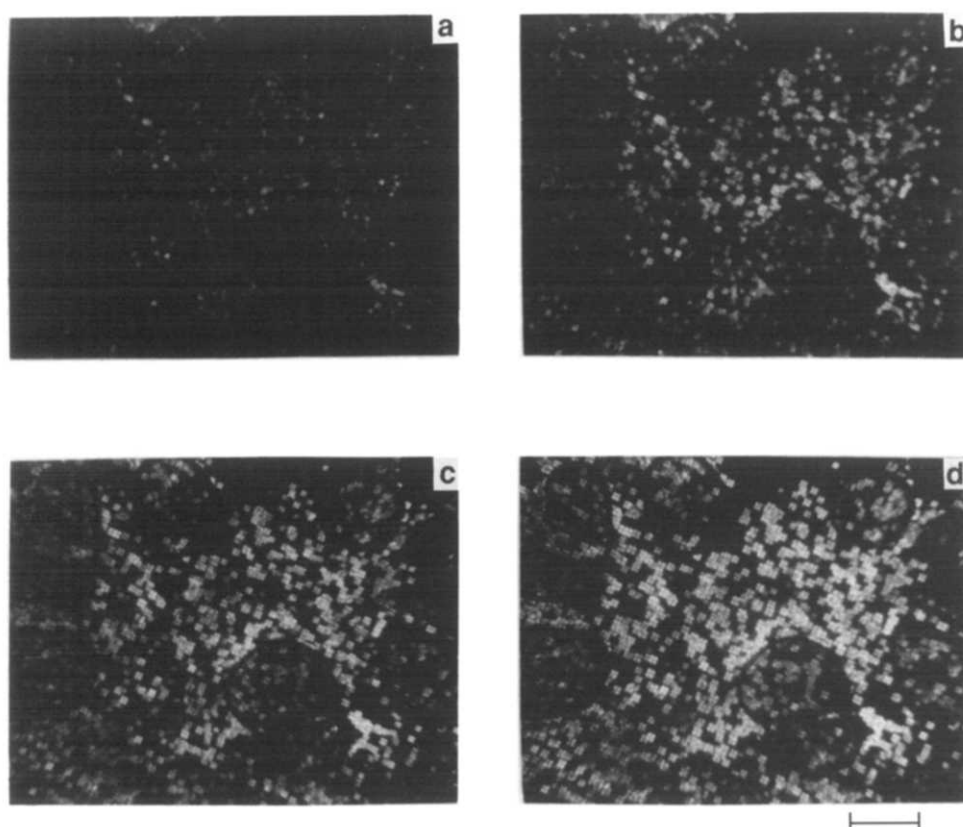


**Figure 2** Optical micrographs showing the evolution of spherulitic growth for sample 1A22/1 with  $M_n = 34\ 900$  after 180 s (a), 205 s (b), 225 s (c) and 240 s (d).  $T_c = 272^\circ\text{C}$ ; scale bar =  $200\ \mu\text{m}$

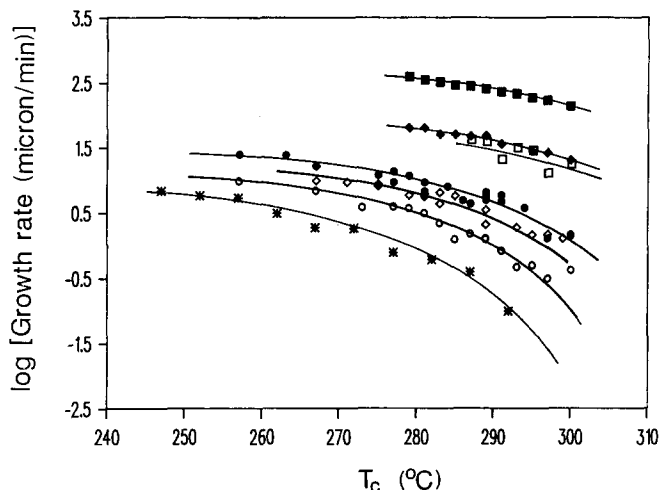


**Figure 3** Dependence of the spherulitic growth rate ( $\mu\text{m s}^{-1}$ ) on crystallization temperature for seven PEEK samples: (■) 2D/1; (□) 1C/1; (●) 2C/1; (●) 1B/1'; (○) 4E/1; (○) 1A22/1; (\*) 4D/1

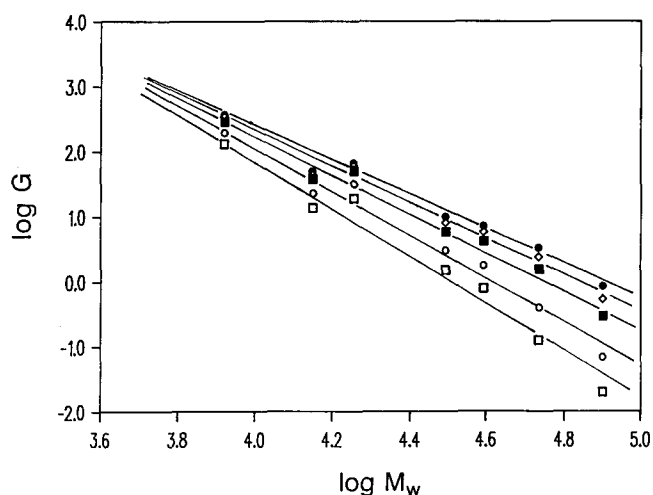


**Figure 4** Log-log plot showing the change in crystal growth rate ( $\mu\text{m s}^{-1}$ ) as a function of molecular weight for different temperatures as extracted from the curves of Figure 3: (□) 295°C; (○) 291°C; (■) 287°C; (○) 283°C; (●) 279°C

recently Hoffman and Miller have proposed, in a more detailed study, that the rate of crystallization depends on  $n^{-1.3}$  for polyethylene fractions near the regime I–regime II transition<sup>16</sup>. A  $M_n^{-1}$  dependence has been observed for *trans*-1,4-polyisoprene<sup>17</sup> and for poly(ethylene terephthalate)<sup>18</sup>.

Other more complex dependences have been proposed. Magill *et al.* arrived empirically at the following equation for poly(tetramethyl-*p*-silphenylene siloxane)<sup>19</sup>:

$$\ln G(T_c) = \text{const.} + BM_n^{-\alpha} \quad (2)$$

where  $0.5 < \alpha < 1.2$ . Cheng and Wunderlich, who studied fractions of poly(ethylene oxide), proposed that for many crystalline polymers<sup>20</sup>:

$$\log G \propto \log(\ln M) \quad (3)$$

This was interpreted to indicate that molecular nucleation rather than secondary nucleation is controlling the crystal growth process. As with the data of Lopez and Wilkes on poly(phenylene sulphide)<sup>14</sup>, we find that the growth rate data plotted according to equation (3) result in downward-tending curves. If a straight line is

forced through the data, a slope of  $-39$  is calculated. It is difficult to propose a physical meaning for this number.

The establishment of empirical relationships like equations (1) to (3) does not provide a precise understanding of the molecular factors that actually influence the spherulitic growth rate, and a more detailed analysis of the data is therefore required. It is generally accepted that the radial growth rate of polymeric spherulites may be expressed as a function of the degree of undercooling from their equilibrium melting point according to the equation of Hoffman *et al.*<sup>21,22</sup>:

$$G = G_0 \exp[-U^*/R(T_c - T_\infty)] \exp[-K_g/T_c(\Delta T)f] \quad (4)$$

where  $G_0$  is a pre-exponential factor that contains all parameters that are only weakly dependent on temperature. The first exponential of equation (4) contains the contribution of diffusional processes to the growth rate, where  $U^*$  is the activation energy for chain diffusion,  $T_\infty$  is the temperature below which such diffusion stops,  $T_c$  is the crystallization temperature, and  $R$  is the gas constant. The value of  $T_\infty = T_g - 55$  has been used in this study. This value is based on the experimentally determined temperature dependence of crystallization rates from the glass determined by d.s.c.<sup>12</sup>. With values of  $T_g$  of each individual sample, values of  $U^*$  ranging from 4140 to 4560 cal mol<sup>-1</sup> were obtained. These two parameters are close to the universal parameters proposed originally by Williams, Landel and Ferry (WLF). It should be pointed out that many authors used  $U^* = 1500$  cal mol<sup>-1</sup> and  $T_\infty = T_g - 30$ , in order to improve the fit with the experimental curve<sup>22,23</sup>. However, in our case, plots of the crystallization rate from the glass as a function of  $T_c - (T_g - 30)$  are slightly curved<sup>12</sup>. From an average slope for each sample,  $U^* = 1765$  to 2155 cal mol<sup>-1</sup> is then obtained. Hoffman *et al.*<sup>22</sup> and Lovinger *et al.*<sup>23</sup> have emphasized the difficulties of deriving the value of the activation energy for spherulitic growth. They have shown that good correlations with the experimental curves can also be obtained with values for  $U^*$  and  $T_\infty$  that are in the vicinity of those used in this study. In addition, experimentally, a value of  $U^* = 4120$  cal mol<sup>-1</sup> has been successfully used for *cis*-1,4-polyisoprene<sup>24,25</sup>. For this reason we have preferred to adhere to a WLF-type equation. The values of  $U^*$  calculated for each sample using either 55 K or 30 K are reported in Table 1.

The second exponential involves the free energy for secondary nucleation and is strongly dependent upon the crystallization temperature  $T_c$  and undercooling  $\Delta T = T_m^\circ - T_c$ , where the equilibrium melting temperature is taken as  $T_m^\circ = 395^\circ\text{C}$ , according to Blundell and Osborn<sup>2</sup>. The factor  $f$  is a correction term that becomes important at high undercooling<sup>22</sup>, which is the case here. Its value is close to unity at high temperature and is given by:

$$f = 2T_c/(T_m^\circ + T_c) \quad (5)$$

From general thermodynamic considerations, the factor  $K_g$  in equation (4) is given by<sup>26</sup>:

$$K_g = \frac{4\sigma\sigma_e T_m^\circ}{\Delta h_f R} \quad (6)$$

where  $\sigma$ ,  $\sigma_e$  and  $\Delta h_f$  are given in cal mol<sup>-1</sup> and  $R$  in cal mol<sup>-1</sup> K<sup>-1</sup>. The numerical factor 4 is specific for

rectangular coherent nuclei<sup>26</sup>. In this form, equation (6) is identical with  $K_g$  of regimes I and III derived from the kinetic theory of crystallization of polymers<sup>22</sup>.

Equations (4) to (6) depend on the value of  $T_m^\circ$ . We have used the value suggested by Blundell<sup>2</sup>,  $T_m^\circ = 395^\circ\text{C}$ , for our initial calculations, although we realize that other values have been suggested<sup>7</sup>. In addition, the dependence of  $T_m^\circ$  on molecular weight is unknown at the present time. In order to examine the effect of a changing  $T_m^\circ$ , we have estimated the values of  $T_m^\circ$  for PEEK samples of different molecular weight based on the dependence observed for poly(phenylene sulphide)<sup>14,23</sup>. We assumed that  $T_m^\circ$  depends on  $M_n^{-1}$  and assigned a value of  $395^\circ\text{C}$  for PEEK with  $M_n = 15000$ . The calculations are described in more details in the previous paper<sup>12</sup>. The calculated values of  $T_m^\circ$  are reported in Table 1.

Equation (4) can be rearranged to:

$$\log G + [U^*/2.303R(T_c - T_g + 55)] = \log G_0 - K_g/2.303T_c(\Delta T)f \quad (7)$$

Consequently, a plot of  $[\log G + U^*/2.303R(T_c - T_g + 55)]$  versus  $[1/T_c(\Delta T)f]$  should yield a straight line with  $\log G_0$  corresponding to the intercept and  $K_g/2.303$  to the negative of the slope. Figure 5 shows these plots for the seven samples described in Table 1. The

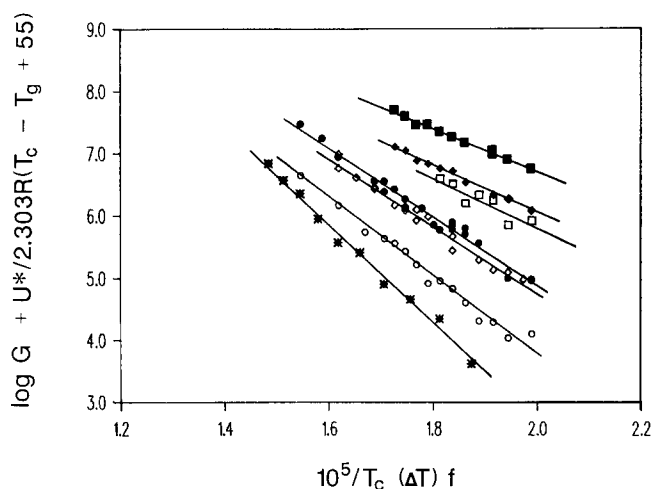


Figure 5 Growth rate data plotted as  $[\log G + U^*/2.3R(T_c - T_g + 55)]$  versus  $[1/T_c(\Delta T)f]$  for various molecular weights: (■) 2D/1; (□) 1C/1; (●) 2C/1; (▲) 1B/1'; (○) 4E/1; (○) 1A22/1; (\*) 4D/1

computation was done using the values  $T_m^\circ = 395^\circ\text{C}$ ,  $T_\infty = T_g - 55\text{ K}$  and  $U^*$  varying between 4140 and 4560 cal mol<sup>-1</sup> (Table 1). Straight lines are obtained in all cases. From the examination of Figure 5, different values for both the slopes and the intercepts are obtained. This suggests that both  $G_0$  and  $K_g$  are functions of molecular weight. The values of  $K_g$  calculated from the slopes are reported in Table 2.

## DISCUSSION

The results of Figure 5 suggest a rather smooth decrease of the slopes and the values of the corresponding  $K_g$  with decreasing molecular weight.

Note that the values of  $K_g$  obtained in this study, e.g. for the high-molecular weight samples ( $\approx 1.8 \times 10^6\text{ K}^2$ ), are lower than the  $K_g$  values obtained from the d.s.c. study ( $\approx 3.0 \times 10^6\text{ K}^2$ )<sup>12</sup>. In view of the widely differing techniques used, we find this reasonable, but it would be more satisfactory if we understood the reasons for this discrepancy. This discrepancy should be kept in mind in the further discussion of the product  $\sigma\sigma_e$  and  $\sigma_e$ .

One can calculate the product  $\sigma\sigma_e$  with equation (5) and the values of  $K_g$  (see Table 2). For the calculations, the values  $\Delta h_f = 130\text{ J g}^{-1}$ ,  $b_0 = 0.468\text{ nm}$  and  $T_m^\circ = 395^\circ\text{C}$  have been taken from the literature<sup>2</sup>. The values for  $\sigma\sigma_e$ , listed in Table 2, increase with molecular weight from 1587 to 3656 erg<sup>2</sup> cm<sup>-4</sup>. For comparison, the values reported for  $\sigma$  and  $\sigma_e$  by Blundell and Osborn for their sample yield  $\sigma\sigma_e = 1862\text{ erg}^2\text{ cm}^{-4}$ , which falls within our interval<sup>2</sup>. The fact that they assume regime I mode of crystallization for their calculation does not change the value since the same numerical factor 4 is used here.

If one assumes that the lateral surface free energy of the lamellae is unlikely to change significantly with respect to molecular weight and that changes in the product can be assigned solely to  $\sigma_e$ , it is possible to estimate  $\sigma_e$  by simply dividing by  $\sigma = 38\text{ erg cm}^{-2}$  (ref. 2). The resulting values, which are listed in Table 2, vary between 41 and 101 erg cm<sup>-2</sup>. Blundell and Osborn obtained  $\sigma_e = 49\text{ erg cm}^{-2}$  from small-angle X-ray scattering<sup>2</sup>. For comparison, the end surface free energy for polyethylene<sup>22</sup> is 90 erg cm<sup>-2</sup>.

In order to see how  $\sigma_e$  changes as a function of molecular weight, we have plotted the logarithm of  $\sigma_e$  against the logarithm of  $M_w$  on Figure 6. A linear plot

Table 2 Calculated values of  $K_g$ ,  $\sigma\sigma_e$  and  $\sigma_e$  based on different values for  $T_m^\circ$  and  $T_x$

Sample	$T_\infty = T_g - 55^\circ\text{C}$ $U^* = 4125\text{--}4500\text{ cal mol}^{-1}$ $T_m^\circ = 395^\circ\text{C}$			$T_\infty = T_g - 30^\circ\text{C}$ $U^* = 1775\text{--}2145\text{ cal mol}^{-1}$ $T_m^\circ = 395^\circ\text{C}$			$T_x = T_g - 55^\circ\text{C}$ $U^* = 4125\text{--}4500\text{ cal mol}^{-1}$ $T_m^\circ$ variable <sup>a</sup>			$T_x = T_g - 30^\circ\text{C}$ $U^* = 4125\text{--}4500\text{ cal mol}^{-1}$ $T_m^\circ$ variable <sup>a</sup>		
	$K_g$ ( $10^6\text{ K}^2$ )	$\sigma\sigma_e$ (erg <sup>2</sup> cm <sup>-4</sup> )	$\sigma_e$ (erg cm <sup>-2</sup> )	$K_g$ ( $10^6\text{ K}^2$ )	$\sigma\sigma_e$ (erg <sup>2</sup> cm <sup>-4</sup> )	$\sigma_e$ (erg cm <sup>-2</sup> )	$K_g$ ( $10^6\text{ K}^2$ )	$\sigma\sigma_e$ (erg <sup>2</sup> cm <sup>-4</sup> )	$\sigma_e$ (erg cm <sup>-2</sup> )	$K_g$ ( $10^6\text{ K}^2$ )	$\sigma\sigma_e$ (erg <sup>2</sup> cm <sup>-4</sup> )	$\sigma_e$ (erg cm <sup>-2</sup> )
4D/1	1.82	3656	101	1.36	2732	70	2.05	4118	105	1.54	3094	79
1A22/1	1.42	2852	73	1.17	2350	60	1.64	3294	84	1.35	2712	69
4E/1	1.26	2531	65	1.00	2009	51	1.43	2872	74	1.11	2230	57
1B/1'	1.27	2552	65	0.97	1948	50	1.38	2772	71	1.06	2129	54
2C/1	0.98	1788	45	0.72	1446	37	0.89	1778	45	0.72	1446	37
1C/1	0.93	1868	48	0.78	1567	40	0.79	1587	41	0.66	1326	34
2D/1	0.79	1587	41	0.62	1245	32	0.59	1185	31	0.46	924	24

<sup>a</sup>See text

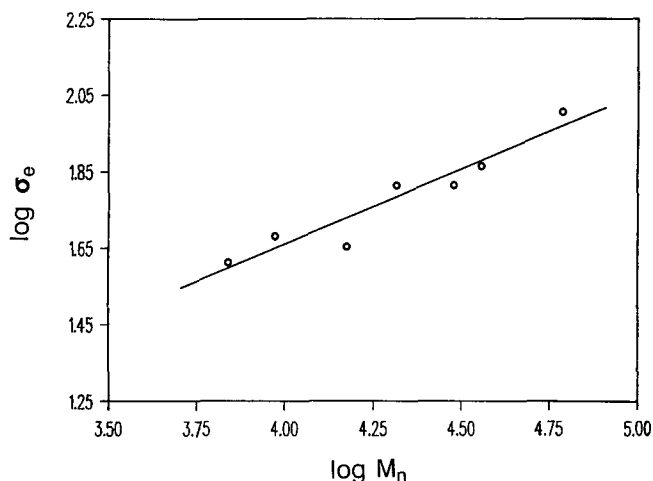


**Figure 6** Dependence of the surface free energy of the PEEK samples as a function of molecular weight, based on the values of  $\sigma_e$  tabulated in the fourth column of Table 2 ( $T_m^\circ = 395^\circ\text{C}$  and  $T_\infty = T_g - 55$ )

with a coefficient of correlation of 0.952 is described by the relation:

$$\sigma_e = AM_w^a \quad (8)$$

A value of  $a = 0.39$  is calculated for the samples studied. It should be pointed out that this relationship holds for the molecular-weight range studied. It is not possible to claim that it would apply to a larger molecular-weight range. The apparent increase in  $\sigma_e$  with molecular weight is often encountered with other polymers<sup>19,27-30</sup> and has been attributed to contributions arising from differences in the perfection of the fold structures of the various samples. In addition, as molecular weight increases, the number of intercrystalline links and chain entanglements becomes relatively more abundant. Those, in turn, affect molecular motion in the polymer melt and so increase the degree of disorder in the intercrystalline region of the crystallized polymer.

We have examined the effect of  $T_\infty$  on the analysis of the data and the values of  $K_g$  and  $\sigma_e$ . It can be seen in Table 2 that a change in  $T_\infty$  from  $T_g - 55$  to  $T_g - 30$ , with a corresponding change in  $U^*$ , decreases  $K_g$  and  $\sigma_e$  by about 20%. In that case, values of  $\sigma_e$  less than  $\sigma = 38 \text{ erg cm}^{-2}$  are observed.

We have also examined the potential effect of using different values for  $T_m^\circ$  for the different molecular weights, since molecular-weight-dependent values of  $T_m^\circ$  have been reported in the literature<sup>7,31</sup>. The effect on the absolute values of the slopes is not negligible, but the trend of the curves is not changed. From Table 2, different values of the slopes (and consequently of  $\sigma_e$ ) are observed, but the relationship between  $M_n$  and  $\sigma_e$  is still obeyed. Actually, a slightly better correlation is obtained when the different values for  $T_m^\circ$  are used.

Another factor that might also have an effect on the calculations of  $\sigma_e$  is the selection of a constant  $\Delta h_f$ . It has been reported that the unit-cell dimensions of PEEK decrease with increasing crystallization temperature<sup>32,33</sup>. This suggests that samples crystallized at different temperatures might be characterized by different values of cohesive energy, which will, in turn, affect their  $\Delta h_f$ . We have used the constant value of  $\Delta h_f = 130 \text{ J g}^{-1}$  for our calculations. Since we suspect that  $\Delta h_f$  is not constant

and changes with  $T_c$ , this value should be considered only as a rough approximation. We do not expect, however, that  $\Delta h_f$  is molecular-weight-dependent.

The representation of the spherulitic growth rate data in Figure 5 is analogous to that of the overall crystallization rate constant  $k$  obtained from the Avrami analysis of the d.s.c. traces, which has been described in the previous paper<sup>12</sup>. Therefore, the results reported here will be combined and their interpretation will be discussed together with those obtained in the d.s.c. study. To summarize, the d.s.c. results have been interpreted as showing two types of behaviour. The higher-molecular-weight samples have a slope of  $K_g/2.303 = -(1.3 \pm 0.1) \times 10^6 \text{ (K}^2\text{)}$ . The low-molecular-weight samples have a slope of  $K_g/2.303 = -(6.0 \pm 0.5) \times 10^5 \text{ (K}^2\text{)}$ . The results for sample 1B/1', with an intermediate molecular weight, are interpreted as consisting of two lines with a slope of  $-1 \times 10^6 \text{ (K}^2\text{)}$  at low temperature and a slope of  $-5.6 \times 10^5 \text{ (K}^2\text{)}$  at high temperature. The ratio of the slopes is about 2 and in agreement with a regime II to III transition. The transition was found at about  $298^\circ\text{C}$ .

Somewhat deliberately, we have interpreted the d.s.c. results of the previous paper<sup>12</sup> as consistent with two regimes and molecular-weight-independent values of  $\sigma_e$ . In contrast, the microscopy data have been interpreted as showing values of  $\sigma_e$  that increase smoothly with molecular weight. These two interpretations are based on two different models for crystallization as given by the two different interpretations of  $K_g$ . The two models are not necessarily mutually exclusive. The question that arises then is whether the data of the d.s.c. work and the microscopy study can be reconciled within one model. It should be noted in this regard that the two techniques do not completely cover the same temperature range. The d.s.c. results of low- $MW$  samples have been obtained above  $300^\circ\text{C}$ . All the microscopy data have been obtained below  $300^\circ\text{C}$ .

The d.s.c. data can all be reconciled within the thermodynamic model presented here. All that is required is that a single line is drawn through the d.s.c. results obtained on 1B/1' and shown in figure 9 of the previous paper<sup>12</sup>. The same  $\sigma_e$  versus  $M_w$  relation is then obtained from the d.s.c. results as shown in Figure 6 for the microscopy results. Within this model it can be argued that if  $\sigma_e$  is molecular-weight-dependent, it is most probably also dependent on the temperature of crystallization, as better crystal surfaces are formed at higher temperature during slower crystallization. No such dependence is found, however, except perhaps in the d.s.c. results of sample 1B/1'. Note that the temperature range covered by each individual sample may be too narrow to observe clearly a temperature dependence.

In order to reconcile all the data within the regime II-regime III kinetic model, we have to assume that the transition temperature between the regimes is molecular-weight-dependent. For the low-molecular-weight samples the transition temperature is presumably below  $280^\circ\text{C}$ . The microscopy data for these samples are then obtained in regime II and the  $\sigma_e$  values for samples 2C/1, 1C/1 and 2D/1 will then be two times those quoted in Table 2 ( $\sigma_e = 82-96 \text{ erg cm}^{-2}$ ). These values of  $\sigma_e$  are then in the range of those obtained for the high-molecular-weight fractions that crystallize in regime III. However, the results indicate that, even if we accept two

regimes, it is found that  $\sigma_e$  increases slightly with molecular weight within regime III.

## CONCLUSIONS

In this work and the previous paper we have explored the crystallization kinetics of poly(aryl ether ether ketone) fractions as a function of molecular weight in the range of 6900 to 60 200 and in the temperature ranges from 145 to 190°C (crystallization from the glass) and 250 to 324°C (crystallization from the melt). The microscopy study is only possible between 250 and 300°C.

The diffusion-controlled crystallization from the glass was discussed in detail in the preceding paper<sup>12</sup>. This analysis was confirmed by a study of the onset of crystallization in a d.s.c. run.

In summary, there are two possible explanations for the observed crystallization rates in the melt. The first would assume no regime model at all and simply invoke that the end surface free energy increases with molecular weight in the temperature and molecular weight ranges studied. This explanation has the undesirable feature that  $\sigma_e \leq \sigma$  for low-molecular-weight samples, although this could be easily changed because the entire evaluation of  $\sigma_e$  given here is based on a single direct measurement of  $\sigma_e$  by Blundell<sup>2</sup>. The second scheme would assume that the regime model is correct; it is then still required that the transition temperature between regimes II and III decreases with decreasing molecular weight. For this point, there is some evidence<sup>25</sup>. Furthermore, we seem to observe small increases in  $\sigma_e$  with increasing molecular weight for the polymers that crystallize in regime III.

## REFERENCES

- 1 May, R. in 'Encyclopedia of Polymer Science and Engineering', Wiley, New York, 1988, Vol. 12, p. 313
- 2 Blundell, D. J. and Osborn, B. N. *Polymer* 1983, **24**, 953
- 3 Kumar, S., Anderson, D. P. and Adams, W. W. *Polymer* 1986, **27**, 329
- 4 Cheng, S. Z. D., Cao, M. Y. and Wunderlich, B. *Macromolecules* 1986, **19**, 1868
- 5 Velisaris, C. N. and Seferis, J. C. *Polym. Eng. Sci.* 1986, **26**, 1574
- 6 Cebe, P. and Hong, S. D. *Polymer* 1986, **27**, 1183
- 7 Lee, Y. and Porter, R. S. *Macromolecules* 1988, **21**, 2770
- 8 Day, M., Suprumchuk, T., Cooney, J. D. and Wiles, D. M. *J. Appl. Polym. Sci.* 1988, **36**, 1097
- 9 Bassett, R. H., Olley, R. H. and Al Raheil, I. A. M. *Polymer* 1988, **29**, 1745
- 10 Deslandes, Y., Day, M., Sabir, F. N. and Suprumchuk, T. *Polym. Compos.* 1989, **10**, 360
- 11 Roovers, J., Cooney, J. D. and Toporowski, P. M. *Macromolecules* 1990, **23**, 1611
- 12 Day, M., Deslandes, Y., Roovers, J. and Suprumchuk, T. *Polymer* 1991, **32**, 1258
- 13 Magill, J. H. *J. Polym. Sci., Polym. Phys. Edn* 1968, **6**, 853
- 14 Lopez, L. C. and Wilkes, G. L. *Polymer* 1988, **29**, 106
- 15 Hoffman, J. D. *Polymer* 1982, **23**, 656
- 16 Hoffman, J. D. and Miller, R. L. *Macromolecules* 1988, **21**, 3038
- 17 Lovinger, E. G. *J. Polym. Sci. (C)* 1970, **30**, 329
- 18 van Antwerpen, F. and van Krevelen, D. W. *J. Polym. Sci., Polym. Phys. Edn* 1972, **10**, 2423
- 19 Magill, J. H. and Li, H.-M. *Polymer* 1978, **19**, 416
- 20 Cheng, S. Z. D. and Wunderlich, B. *J. Polym. Sci., Polym. Phys. Edn* 1986, **24**, 595
- 21 Hoffman, J. D. and Lauritzen, J. I. *J. Res. Natl. Bur. Stand. (A)* 1961, **65**, 297
- 22 Hoffman, J. D., Davis, G. T. and Lauritzen, J. I. in 'Treatise on Solid-State Chemistry' (Ed. N. B. Hannay), Plenum Press, New York, 1976, Vol. 3, Ch. 7
- 23 Lovinger, A. J., Davis, D. D. and Padden, F. J., Jr *Polymer* 1985, **26**, 1595
- 24 Dalal, E. N. and Phillips, P. J. *J. Polym. Sci., Polym. Lett. Edn* 1984, **22**, 7
- 25 Phillips, P. J. and Vatansver, N. *Macromolecules* 1987, **20**, 2138
- 26 Stack, G. M., Mandelkern, L., Krohnke, C. and Wegner, G. *Macromolecules* 1989, **22**, 4351
- 27 Devoy, C. and Mandelkern, L. *J. Polym. Sci. (A-2)* 1969, **7**, 1883
- 28 Phillips, P. J., Rensch, G. J. and Taylor, K. D. *J. Polym. Sci. (B) Polym. Phys.* 1987, **25**, 1725
- 29 Garza, J., Fatou, J. G. and Bello, A. *Polymer* 1981, **22**, 477
- 30 Marco, C., Fatou, J. G. and Bello, A. *Polymer* 1977, **18**, 1100
- 31 Hoffman, J. D. *Polymer* 1983, **24**, 3
- 32 Hoffman, J. D. and Weeks, J. J. *J. Res. Natl. Bur. Stand. (A)* 1962, **66**, 13
- 33 Cebe, P. *J. Mater. Sci.* 1988, **23**, 3721
- 34 Wakelyn, N. T. *J. Polym. Sci. (C) Polym. Lett.* 1987, **25**, 25
- 35 Hay, J. N., Langford, J. I. and Lloyd, J. R. *Polymer* 1989, **30**, 489